JOURNAL OF MATERIALS SCIENCE 31 (1996) 881–893

Effects of heat treatments on the microstructure of a superplastic Ti_3Al based alloy

D. JOBART, J. J. BLANDIN
Institut National Polytechnique de Grenoble, Génie Physique et Mécanique des Matériaux, ENS de Physique de Grenoble, Unité de Recherche Associée au CNRS No. 793, BP 46–38 402, Saint-Martin d'Hères Cedex, France

The ability to develop superplastic properties in a two phase material depends mainly on three physical features: the volume fraction of the phases, their size (and morphology) and their composition (associated with their crystallographic structure). All these parameters are functions of the temperature of deformation. Therefore, their variation with temperature is required to determine the temperature domain in which superplastic properties can be expected and then to investigate the mechanisms of deformation induced in the superplastic regime. The material investigated in this study is an industrial Ti_3Al based alloy, to be formed by superplastic forming. From microstructural characterization of the material in as-received conditions, it is concluded that superplastic properties can be achieved with the provided microstructure. Microstructural transformation (variations in phase compositions, grain sizes and crystallographic structure) associated with annealing in the temperature range 890–1070 °C was investigated. The law of variation with temperature of phase volume fractions was determined by two independent methods.

1. Introduction

The Ti_3Al titanium aluminide based alloys show mechanical properties which make them attractive candidates for aeronautical components in place of conventional titanium alloys, such as Ti–6Al–4V (wt %). However, these materials generally exhibit low ductilities requiring one to optimize shape forming techniques. Consequently, the achievement of superplastic properties has received increasing attention in the last few years to produce structural parts by superplastic forming of sheets.

Superplastic deformation of Ti_3Al based alloys was firstly reported in 1990 [1] in the case of a regular Ti–24Al–11Nb (at %) alloy (referred as α_2 alloy) and was increasingly investigated until now, particularly in the case of the Ti–25Al–10Nb–3V–1Mo (at %) alloy (referred as super α_2 alloy) [2–5]. Large elongations to rupture have been obtained (up to 800%) for a deformation temperature close to 980 °C for both alloys. At this temperature, the Ti_3Al titanium aluminide based alloys are in the two phase ($\alpha_2 + \beta$) field.

In the case of conventional titanium alloys, elongation to rupture in superplastic conditions has been demonstrated to result mainly from three microstructural features: the volume fraction of the phases, their mean size (and shape) and their composition.

In the case of the Ti–6Al–4V (wt %) and Ti–6Al–2Sn–4Zr–2Mo (wt %) alloys, maximum elongations were demonstrated to coincide with approximately equal phase proportions [6]. This result was confirmed for other conventional titanium alloys [7]. For too large an α-phase volume fraction, superplastic deformation requires significant mechanical contribution of this phase, which is considered as the hard phase of the alloy, since diffusion coefficients in the α-phase are generally at least two orders of magnitude lower than those in the β-phase, in the temperature domain in which superplastic properties can be achieved. For too large a β-phase volume fraction, excessive growth of β grains takes place during deformation, which leads to the development of microstructures which are incompatible with superplastic conditions.

In the case of the Ti–24Al–11Nb (at %) alloy, superplastic properties can be maintained for materials containing significantly larger volume fractions of the hard α_2-phase [1]. Elongations to rupture close to 400% were reported for alloys containing about 75 vol % α_2-phase. For the Ti–25Al–10Nb–3V–1Mo (at %) alloy, the relation between elongation to rupture and phase volume fractions was not precisely determined, since the law of variation of the phase volume fractions with temperature is not yet well established.

Since grain (or phase) boundary sliding is the main mechanism of superplastic deformation, superplastic properties require a fine microstructure. In the case of two phase materials, a mean grain size of about 5 μm or less is generally required. The grain size is thus produced by a thermomechanical process, which includes hot working and recrystallization steps.

For a given phase volume fraction, the composition of the phases have been demonstrated to play a key role in the ability to develop superplastic properties in

0022–2461

conventional titanium alloys [6, 8, 9]. Wert and Paton [8] have shown that the addition of some solutes in the alloy, like iron, cobalt or nickel, can enhance superplastic properties. These solutes have diffusion coefficients in the β-phase significantly larger than the corresponding diffusion coefficient of titanium. Since the deformation rate is closely related to diffusion kinetics in the softer phase in the case of superplastic deformation of a two phase material [10], the introduction of these solutes allows a significant decrease of the temperature range in which a superplastic regime can be achieved. Moreover, it must be kept in mind that, even for a constant nominal composition of an alloy, the compositions of the phases vary with temperature. Such variations in compositions can result in significant variations in diffusion kinetics.

From a mechanical point of view, it has been well established that elongation to rupture is closely related to the value of the strain rate sensitivity parameter, m, as defined by the conventional viscoplastic law, $\sigma = K\dot{\varepsilon}^m$, where σ is the flow stress, $\dot{\varepsilon}$ the strain rate and K a metallurgical parameter. The largest elongations to rupture coincide with the largest values of m. In the case of conventional titanium alloys, it has been demonstrated that the addition of fast diffusing solutes results in an increase of the strain rate sensitivity parameter in the superplastic regime [8].

In order to understand the physical mechanisms which are induced during superplastic deformation of the Ti–25Al–10Nb–3V–1Mo (at %) alloy, it is of prime importance to obtain a correlation between the m values and the microstructural transformations which can be induced during heat treatment of the as-received material at different temperatures. This is the main purpose of this paper. After a short presentation of the superplastic properties of the investigated material, the paper focuses on the microstructural characterization of the as-received material and on the effect of heat treatment on the size, morphology and composition of the phases. The expected consequences on superplastic properties are then discussed.

2. Experimental procedure

The material used in this study was obtained from TIMET Corporation as hot rolled sheets of 3 mm thickness. The nominal composition of the alloy is Ti–24.4–Al–10.6Nb–3.0·V–1.0Mo (at %) and the oxygen content is 800 p.p.m., as given by the supplier. The processing route is not known in detail. Nevertheless, it can be assumed that the material was initially rolled in the β field and then in $\alpha_2 + \beta$ domain in order to obtain a fine two phase microstructure.

Scanning electron microscopy (SEM) was carried out on mechanically polished and etched specimens (8% HNO_3, 2% HF, 90% H_2O). Phase area fractions were measured by image analysis performed on SEM micrographs and the grain size (GS) was estimated from linear intercept measurements. Each intercept corresponds to an α_2–β interface, and consequently does not take into account the α_2–α_2 and β–β boundaries. Measurements were carried out in three planes of observation: the sheet plane (P1) and the two perpendicular cross-sectional planes (P2 and P3). In each plane of observation, mean intercepts were measured along several directions, allowing the determination of a minimum or maximum L_i^{min} or L_i^{max}, respectively, intercept. From the quantification of these intercept measurements, some assumptions concerning the shape of the grains have been made to allow the calculation of GS. These assumptions will be detailed later.

X-ray diffraction analysis was performed using a CuK_α radiation diffractometer. Analyses were carried out in the sheet plane (P1) and in cross-sections (P2 and P3) to identify the phases and to obtain data about the texture of the α_2 and β-phases. Phase compositions were measured by wavelength dispersive spectroscopy (WDS). Each reported phase composition is the mean value of at least five analyses, instead of which were performed, as far as possible, in the centre of each phase to limit the contribution of the other one. Pole figures limited to 75° tilt were measured on a texture goniometer using CuK_α radiation. The pole intensities were normalized by integrating over the whole measured range and dividing the particular intensity of one pole figure point by this integral value.

Heat treatment was carried out in air at 890, 920, 950, 980, 1010, 1030, 1050, 1070, 1090 and 1110 °C. After each treatment, the samples were water quenched. The corresponding cooling rate was estimated to be 50 °C s^{-1}. The duration of the treatments was 24 h. Mechanical testing at high temperature was carried out in tension under an argon atmosphere in the temperature range 850–1100 °C for various strain rates within the interval 5×10^{-5} s^{-1} to 5×10^{-3} s^{-1}. The deformation temperature was achieved in approximately 1 h, and 30 min were required to homogenize the temperature in the vicinity of the sample.

3. Results

3.1. Superplastic properties

The superplastic properties were estimated from velocity change tests. Fig. 1 shows the variation with temperature of the strain rate sensitivity parameter, m, for a strain rate of 5×10^{-4} s^{-1}. Maximum values, close

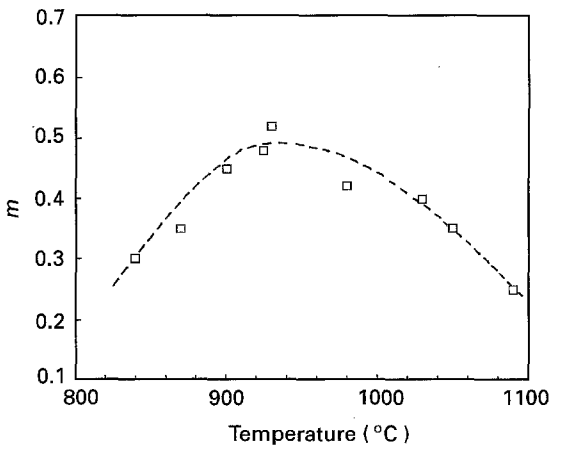

Figure 1 Variation with temperature of the strain rate sensitivity parameter, m, for a strain rate equal to 5×10^{-4} s^{-1}.

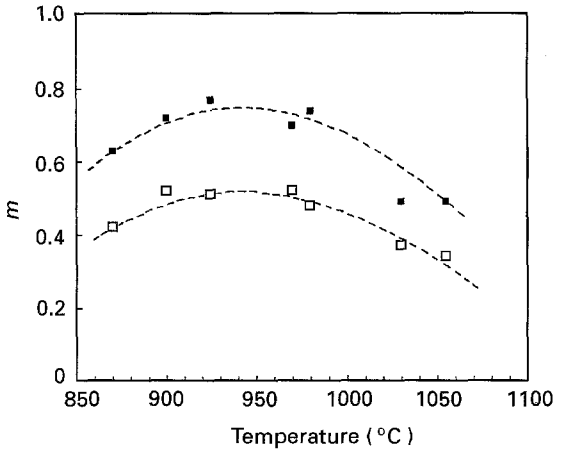

Figure 2 Variation with temperature of the (□) minimum and the (■) maximum values of the strain rate sensitivity parameter, m, in the investigated strain rate domain.

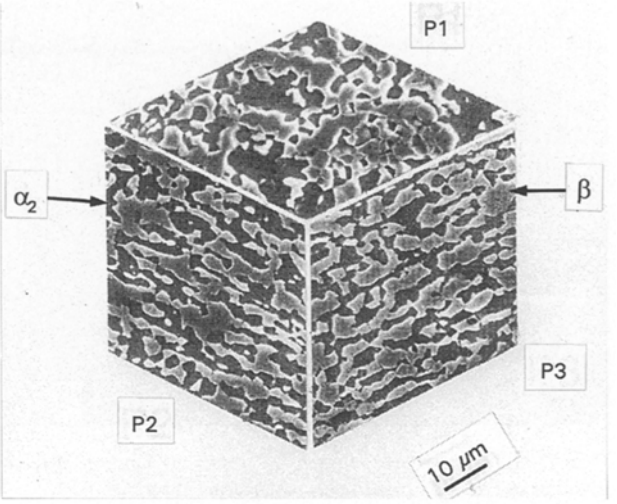

Figure 3 SEM micrograph showing the three-dimensional microstructure of the as-received material.

to 0.5, are obtained in the temperature range 930–980 °C. These results are in agreement with previous studies on the Ti–25Al–10Nb–3V–1Mo (at %) alloys [2–5], for which the optimum temperatures for superplasticity ranged from 950 to 980 °C. It is also confirmed by Fig. 2, which shows the variation with temperature of the minimum and maximum values of m in the investigated strain rate domain. The best superplastic rheologies were still obtained in the temperature domain 930–980 °C. A maximum value of m of about 0.7 was observed at a temperature of 930 °C for a strain rate of 5×10^{-5} s^{-1}.

3.2. Microstructure of the as-received material

3.2.1. Phase size and morphology

Fig. 3 shows the three-dimensional microstructure of the as-received material. The microstructure consists of a fine mixture of α_2 and β-phases. In the sheet plane (P1), $L_1^{min} \approx L_1^{max}$, which means that the microstructure can be considered as equiaxed in this plane. This observation indicates that the material was cross rolled, at least partially. This result was confirmed by the fact that in the cross-sectional planes (P2 and P3), $L_2^{max} \approx L_3^{max} \approx L_1^{max}$ and $L_2^{min} \approx L_3^{min}$. These results show that the microstructure can be modelled as a pile-up of parallelepipeds defined by the lengths L_2^{max}, L_2^{max} and L_2^{min}. Consequently, the phase size (PS) is defined as

$$PS = [L_2^{min}(L_2^{max})^2]^{1/3} \quad (1)$$

For the as-received material, PS = 3.4 μm. In the sheet plane as well as in cross-sections, both phases have comparable phase sizes, i.e. $PS_{\alpha_2} \approx PS_\beta \approx PS$. As already mentioned, the linear intercepts take into account only α_2/β interfaces, therefore overestimating the actual grain size. This overestimation can be roughly determined in the case of the β grains, since an intergranular precipitation occurs along β–β boundaries during the cooling step which followed the last rolling step. The intergranular phase has been demonstrated to be the α_2-phase [11]. From Fig. 4 and some

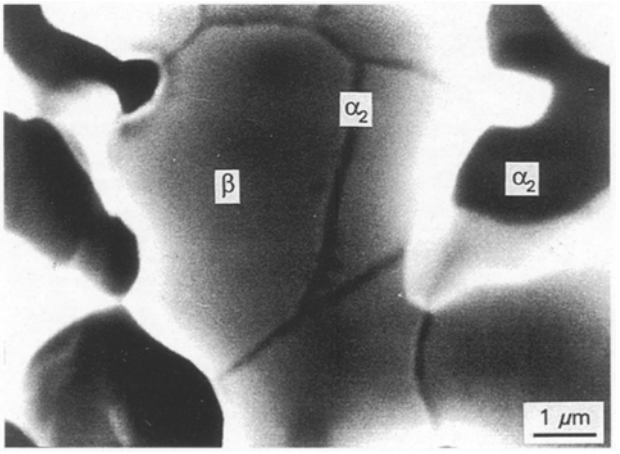

Figure 4 SEM micrograph of the precipitation of α_2-phase along β–β boundaries in the as-received material.

other additional SEM observations, it can be deduced that the β grain size GS_β is roughly equal to $PS_\beta/2$, namely less than 2 μm. Such a β-phase size has been demonstrated to be compatible with superplastic deformation in the case of the Ti–25Al–10Nb–3V–1Mo (at %) alloy [2, 3], assuming that the experimental conditions (temperature and strain rate) do not strongly affect this microstructure.

3.2.2. Phase volume fraction

Attention must be drawn to the relative inhomogeneity in phase distribution which has been detected in the sheet plane, as illustrated by Fig. 5: large zones of α_2- or β-phase agglomeration having sizes larger than 20 μm are observed. These heterogeneities appear systematically in planes near the surface, as well as in the centre of the sheet. Therefore, phase volume fractions were measured by image analysis performed in cross-sectional planes and a satisfactory phase distribution homogeneity was observed from the surface to the centre of the sheet.

It has been extensively reported that, despite efforts to limit the presence of air in contact with the sheet

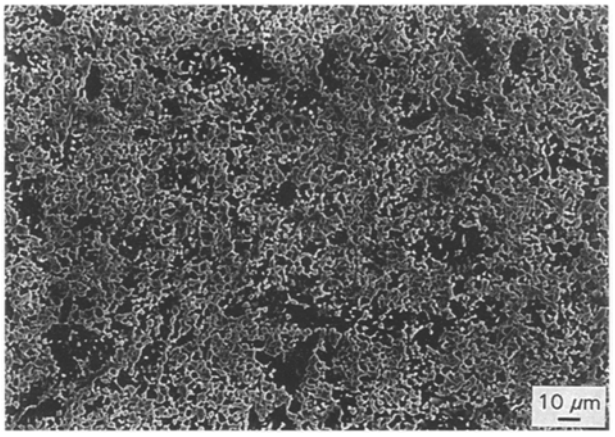

Figure 5 SEM micrograph showing phase distribution heterogeneities in the sheet plane of the as-received sheet.

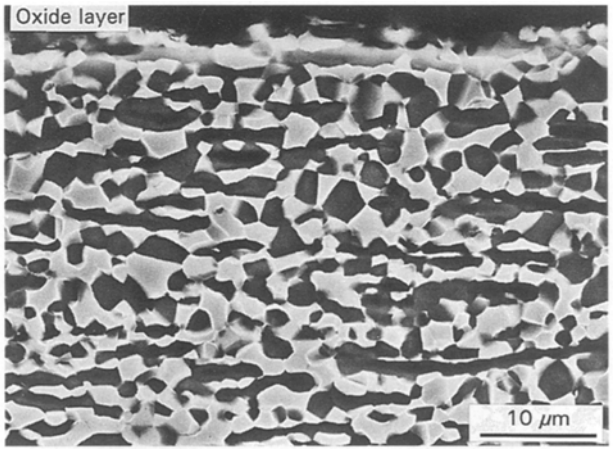

Figure 6 SEM micrograph of the zone under the surface of the sheet, observed in cross-section.

during hot rolling of titanium aluminides, an oxide layer is generally observed at the surface of the material, associated with possible oxygen contamination of the material in a region located just under the surface. In the case of the investigated material, an oxide was indeed detected at the surface of the sheet. It has been identified mainly as TiO_2, in association with other oxides containing aluminium and niobium. As a result of the strong effect of oxygen concentration on the phase volume fractions and β transus temperature in titanium aluminides [12, 13], a local increase in α_2 volume fraction can then be expected near the surface. This point has been checked and, as illustrated by Fig. 6, no significant contamination zone is observed in the investigated material and the volume fraction of the α_2-phase is nearly constant through the cross-section. In the as-received conditions, an α_2-phase volume fraction $f_{vol}(\alpha_2) \approx 50\%$ is obtained. Since the two phases have quite similar sizes, both phases are likely to be connected.

3.2.3. X-ray diffraction results

Fig. 7a–c shows X-ray diffraction spectra of the as-received alloy, performed in the three planes already defined (P1, P2 and P3). Whatever the plane of analysis, most of the peaks can be attributed to the hexagonal $D0_{19}$ structure of the α_2-phase or to the cubic structure of the β-phase. However, the amplitude of the peaks depends strongly on the analysis plane. Concerning the β-phase, the (2 0 0) peak is predominant when the spectrum is performed in the sheet plane (P1), whereas the (1 1 0) peak is preferentially present when the analysis is carried out in cross-section (P2 or P3). Concerning the α_2-phase, differences in spectra are also obtained, but to a smaller extent: $(2\,2\,\bar{4}\,0)$ peaks are predominant in the sheet plane, whereas the (0 0 0 2) peak is preferentially obtained in cross-section. Since X-ray diffraction profile can provide first-order approximation of the texture of the alloy, it can be deduced that a texture is present in α_2- and β-phases in the as-received conditions. To quantify it, {2 0 0} and $\{2\,2\,\bar{4}\,0\}$ pole figures have been obtained from the as-received titanium aluminide sheet and are presented in Fig. 7d, e. They confirm the (1 0 0) [0 1 1] component for the β-phase. For the α_2-phase, two textural components $(1\,1\,\bar{2}\,0)$ $[\bar{1}\,1\,0\,0]$ and $(1\,1\,\bar{2}\,0)$ [0 0 0 1] are observed.

Particular attention has been drawn to detect the presence of both the ordered B2 and the orthorhombic

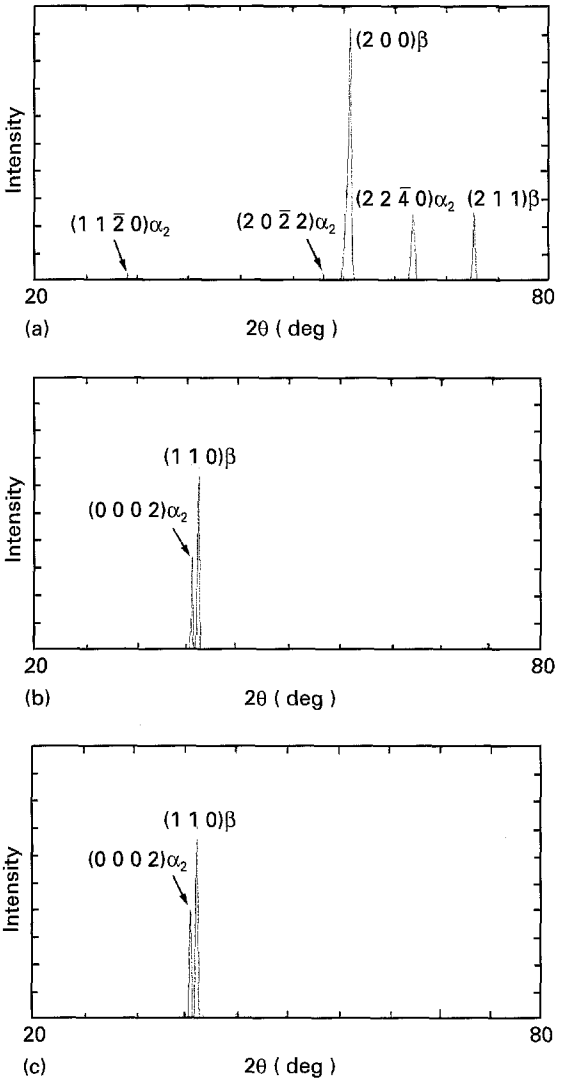

Figure 7 X-ray diffraction spectra of the as-received material: (a) analysis in the sheet plane, (b) and (c) analysis in cross-section, (d) {2 0 0} β pole figure of the as-received alloy, and (e) $\{2\,2\,\bar{4}\,0\}$ α_2 pole figure of the as-received alloy.

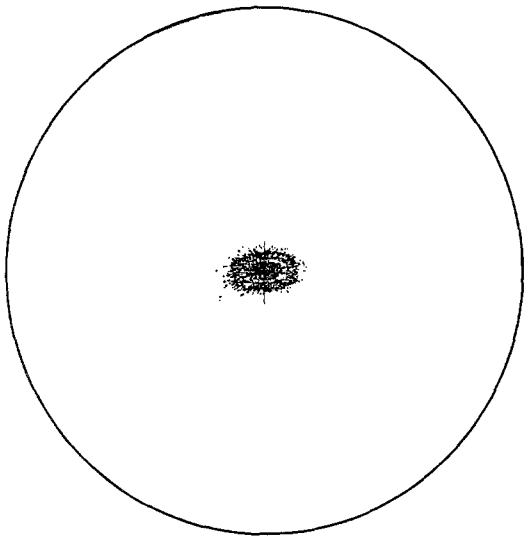

(d)

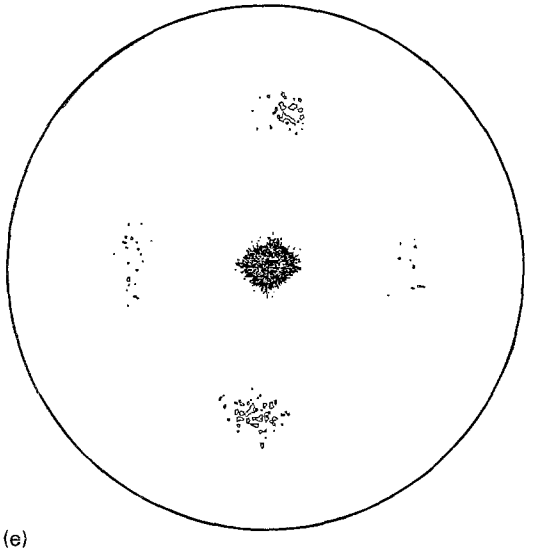

(e)

Figure 7 (Continued)

structures in the as-received alloy, which have been already reported in the case of Ti_3Al based alloys [14, 15]. When the B2 phase is present, the superlattice (1 0 0) peak can be observed for $d \approx 0.324$ nm [14]. On the X-ray spectrum performed from $2\theta = 20$–$40°$ in the sheet plane of the as-received material (Fig. 8), B2 structure is detected but the intensity of the peak remains very limited, which means that ordering of the β-phase is not complete in the as-received condition. The orthorhombic phase can be detected by X-ray diffraction analyses since a double peak then appears in the vicinity of the (1 0 $\bar{1}$ 1) peak of the α_2-phase: this second peak corresponds to the (1 1 1) peak of the orthorhombic phase. On Fig. 8, a peak is observed very close to the (1 0 $\bar{1}$1) α_2 peak. It corresponds to $d = 0.335$ nm. Morris and Morris [14] have measured the lattice parameters of the orthorhombic phase in a Ti–24Al–11Nb–2V–1Mo (at %) alloy and found $a = 0.595$ nm, $b = 0.985$ nm and $c = 0.450$ nm. If these lattice parameters are used to calculate d(1 1 1) of the orthorhombic phase, it yields

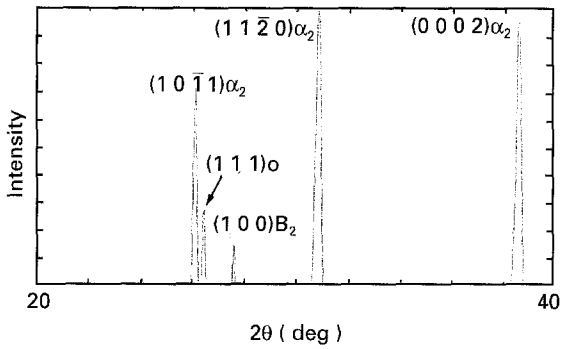

Figure 8 Expanded scale between 20 and 40° of X-ray diffraction spectrum of the as-received alloy in the sheet plane.

TABLE I WDS analysis of global, α_2 and β composition in the as-received alloy

Elements (at %)	Ti	Al	Nb	V	Mo
Global	61.2	24.1	10.6	3.0	1.0
α_2	63.8	24.9	8.9	2.1	0.4
β	58.5	22.4	12.7	4.5	1.9

d(1 1 1) = 0.337 nm, which is in relatively good agreement with the experimental peak. Consequently, some orthorhombic phase is considered to be present in the as-received alloy.

3.2.4. Phase composition

Table I summarizes the global composition of the alloy and the α_2- and β-phase compositions, obtained from WDS measurements. The nominal composition given by the supplier is confirmed. As expected, niobium, vanadium and molybdenum are concentrated in the β-phase, whereas the α_2-phase contains preferentially aluminium and titanium. It must be noted that WDS measurements performed in the β-phase are likely to include the contribution of α_2 precipitates which nucleate along β–β boundaries. Nevertheless, since these precipitates appear during cooling after the last rolling step, the WDS results are representative of the composition of the β-phase during the last rolling step performed at high temperature.

3.3. Effect of heat treatment

3.3.1. Effect on phase morphology and size

Fig. 9a–f shows SEM micrographs of the specimens, heat treated in the temperature range 890–1050 °C, observed in cross-section. When the specimens are heat treated at a temperature higher than 1050 °C, as α_2-phase is no longer observed throughout the microstructure.

1. Heat treatment at $T < 1000$ °C: when heat treatment is performed at a temperature lower than 1000 °C (Fig. 9a–c), the global morphology of the alloy is only slightly affected. The microstructures can then be correctly described with PS and the two phases can still be considered as two connected networks. Fig. 10 shows the variation with temperature

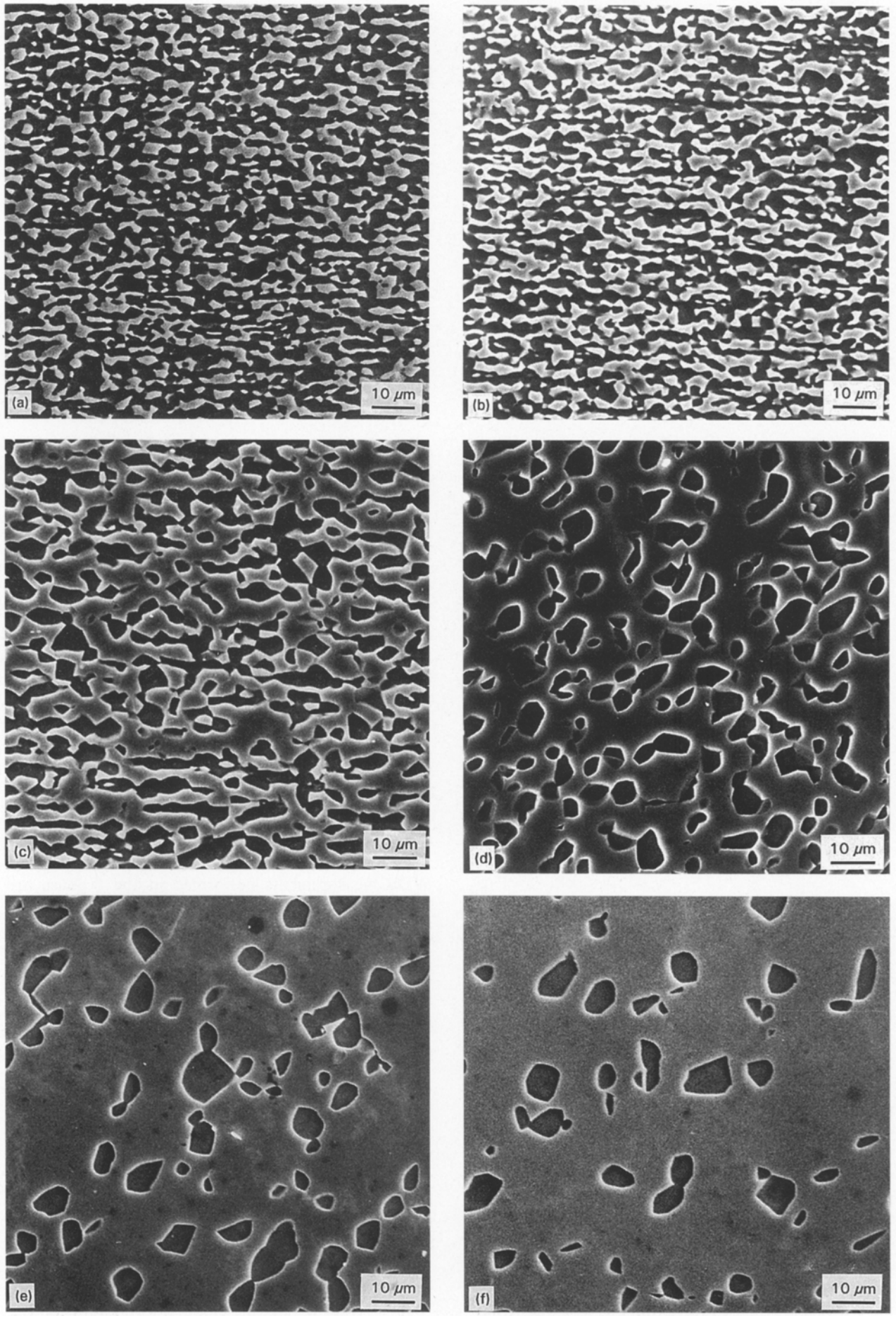

Figure 9 SEM micrographs of heat treated specimens observed in cross-section: (a) $T = 890\,^{\circ}C$, (b) $T = 920\,^{\circ}C$, (c) $T = 980\,^{\circ}C$, (d) $T = 1010\,^{\circ}C$, (e) $T = 1030\,^{\circ}C$, and (f) $T = 1050\,^{\circ}C$.

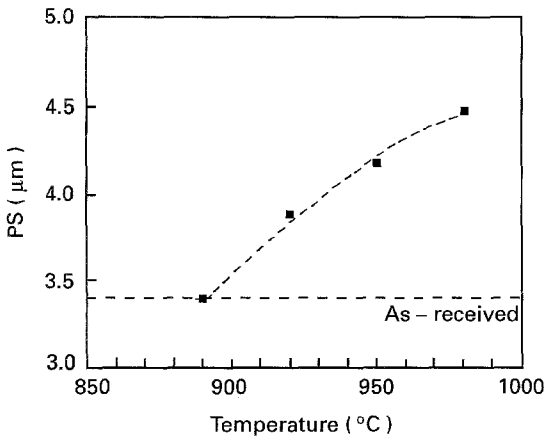

Figure 10 Variation with temperature of treatment of the phase size (PS).

of the phase size (PS), as defined in Equation 1. PS increases with increasing temperature. Nevertheless, grain growth remains limited even for the highest temperature ($T = 980\,°C$). This result shows that the important grain growth usually reported [4] after superplastic deformation performed at 980 °C must be mainly attributed to dynamic grain growth rather than static grain growth. Whatever the temperature of treatment, the preferential orientation of the microstructure is roughly maintained. This preferential orientation is, however, slightly reduced when the material is heat treated at 980 °C (Fig. 9c), which can be attributed to thermally activated diffusion processes which tend to spheroidize the α_2 nodules in order to reduce, as much as possible, the interface area in the material.

2. Heat treatment at $T > 1000\,°C$: when heat treatment is performed at a temperature higher than 1000 °C (Fig. 9d–f), the microstructure is deeply affected. The α_2-phase is no longer connected and a dispersion of α_2 nodules in the continuous β-phase is formed. In this context, PS is no longer a relevant parameter to describe the microstructure. The continuous decrease in α_2 volume fraction is associated with the increase in temperature. It results preferentially from a reduction of the density of α_2 nodules rather than of their mean size. This means that shrinkage and coalescence occur simultaneously during the performed heat treatments. However, attention has to be drawn to the fact that oxygen contamination is likely to take place through the samples treated in the upper domain of the investigated temperature range, namely at $T \geqslant 1050\,°C$. As already mentioned, such enrichment in oxygen is expected to promote the development of the α_2-phase and then to affect estimation of its volume fraction, namely to overestimate it.

3.3.2. Effect on the crystallography of the phases

Fig. 11 shows the X-ray spectra of a specimen heat treated for 24 h at 980 °C, when the analysis is carried out in the sheet plane (Fig. 11a) and in cross-section (Fig. 11b). The same peaks are detected in all the X-ray spectra performed from $2\theta = 20$ to 80° when the heat treatment temperature ranges from 890 to 1050 °C. As obtained for the as-received alloy, the (2 0 0) [respectively, (2 2 $\bar{4}$ 0)] peak is predominant in the sheet plane, whereas the (1 1 0) [respectively, (0 0 0 2)] peak is preferentially present in cross-section for the β and α_2 phases. These results suggest that the initial texture is roughly maintained in the material after heat treatment performed in the investigated temperature range. To confirm this result, {2 0 0} and {2 2 $\bar{4}$ 0} pole figures have been measured for specimens heat-treated for 24 h at 980 °C. They are presented in Fig. 11c. The textural components obtained in the as-received conditions (see Fig. 7d, e) are still present after heat treatment: (1 0 0) [0 1 1] for the β-phase and (1 1 $\bar{2}$ 0) [$\bar{1}$ 1 0 0] and (1 1 $\bar{2}$ 0) [0 0 0 1] for the α_2-phase. Therefore, it can be concluded that whatever the temperature of superplastic deformation, a significant texture in both phases will be present in the alloy when deformation starts. From X-ray spectra obtained in the sheet plane of the heat treated specimens, the superlattice (1 0 0) peak of the B2 phase is still detected after annealing, as confirmed by Fig. 11d, but its intensity remains very limited, which means, as it was obtained in the as-received condition, that ordering is not complete. This result is in agreement with calculations of the long range order parameter of Ti–24Al–11Nb–2V–1Mo (at %) specimens heat treated in a similar way as in this study [14]. For materials treated in the range 900–1000 °C, the value of the calculated long range order parameter was quite small (about 0.3).

After treatment and in the whole investigated temperature domain, the orthorhombic phase is no

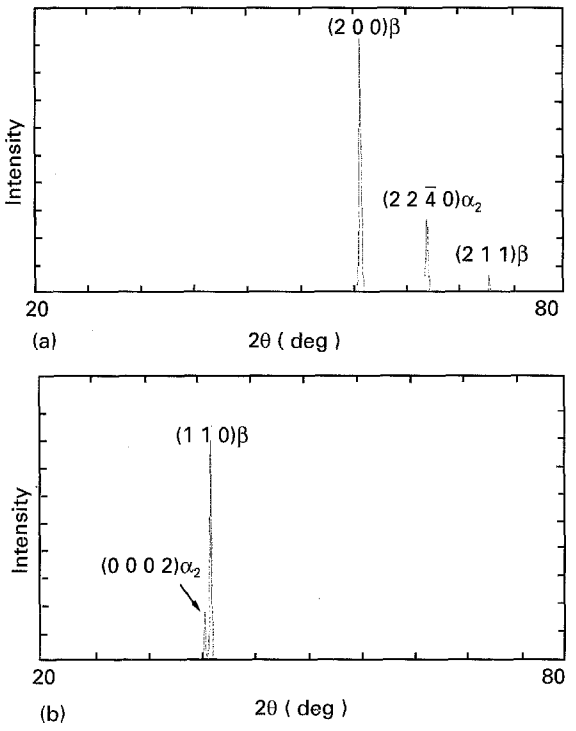

Figure 11 X-ray spectrum in: (a) the sheet plane of heat treated specimen (980 °C, 24 h), (b) a cross-section of heat treated specimen (980 °C, 24 h), (c) {2 0 0} β and {2 2 $\bar{4}$ 0} α_2 pole figures of heat treated specimen (980 °C, 24 h), and (d) expanded scale between 20 and 40° in the sheet plane of heat treated specimen (980 °C, 24 h).

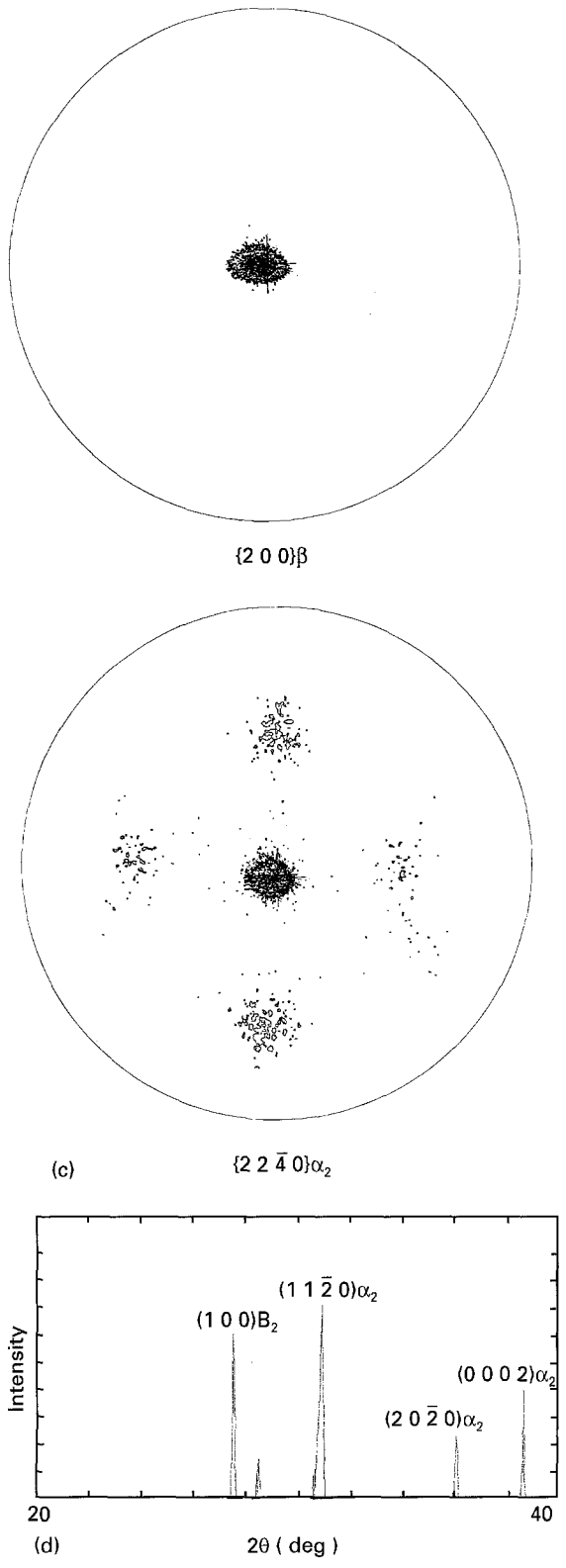

Figure 11 (Continued)

longer detected. This result is again in agreement with the study performed by Morris and Morris [14].

3.3.3. Effect on phase volume fractions

From image analysis data, the variation with temperature of the α_2 volume fraction, $f_{vol}(\alpha_2)$, has been measured, as shown in Fig. 12. $f_{vol}(\alpha_2)$ remains relatively constant at low temperatures ($T < 960\,^{\circ}C$) and decreases thereafter. As already mentioned, since oxygen contamination occurred during heat treatment

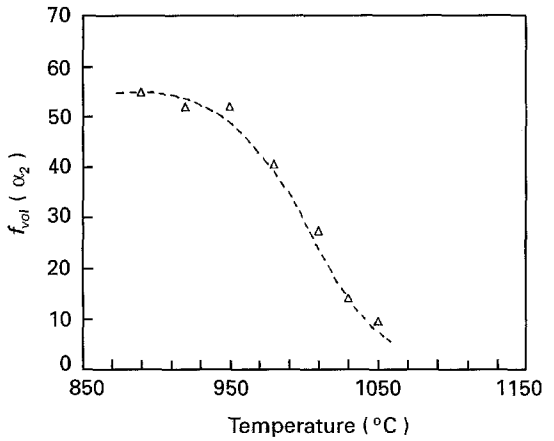

Figure 12 Variation with temperature of $f_{vol}(\alpha_2)$ from data obtained by image analysis.

at $T \geqslant 1050\,^{\circ}C$, the actual value of $f_{vol}(\alpha_2)$ at $T = 1050\,^{\circ}C$ can be slightly overestimated and the amplitude of this overestimation is difficult to estimate. Nevertheless, the β transus temperature, T_β, for the investigated alloy is close to 1070 °C, in good agreement with previously reported values of T_β [16, 17].

3.3.4. Effect on phase composition

The effect of heat treatment on phase composition was quantified by WDS measurements performed on quenched specimens. It was assumed that no variation in phase composition occurs during water quenching. This hypothesis is in agreement with results obtained in the case of a Ti–23Al–3Mo (at %) alloy, for which phase compositions were demonstrated to significantly depend on cooling rate after heat treatment at the β transus temperature of the alloy (in that case, $T_\beta \approx 1030\,^{\circ}C$), only when the cooling rate was less than $5\,^{\circ}C\,s^{-1}$ [18]. It must be kept in mind that during the performed water quench, a cooling rate of about $50\,^{\circ}C\,s^{-1}$ was estimated.

Fig. 13a–e shows the variation of the composition of the α_2- and β-phases with temperature. For all the investigated elements, the compositions of the two phases are on both sides of the nominal composition of the alloy and when $T > 1050\,^{\circ}C$, the measured composition of the β-phase is in good agreement with the nominal composition of the alloy, particularly for the β stabilizing elements. In the case of titanium and aluminium, and whatever the temperature of treatment, the relative differences in compositions between the two phases are very limited (the maximum ratio between the amounts in the α_2- and β-phases is less than 1.2). In the case of the β stabilizing elements, the differences in composition between the α_2- and β-phases are more pronounced (from a maximum of 1.7 for niobium and 2.8 for vanadium, to 13 for molybdenum). For these three solutes, the dependence on temperature of the α_2 composition is very limited. This is particularly the case for molybdenum, as a result of its low solid solubility limit in the hexagonal $D0_{19}$ structure. Therefore, variation of phase composition occurs mainly in the β-phase. As expected, a common

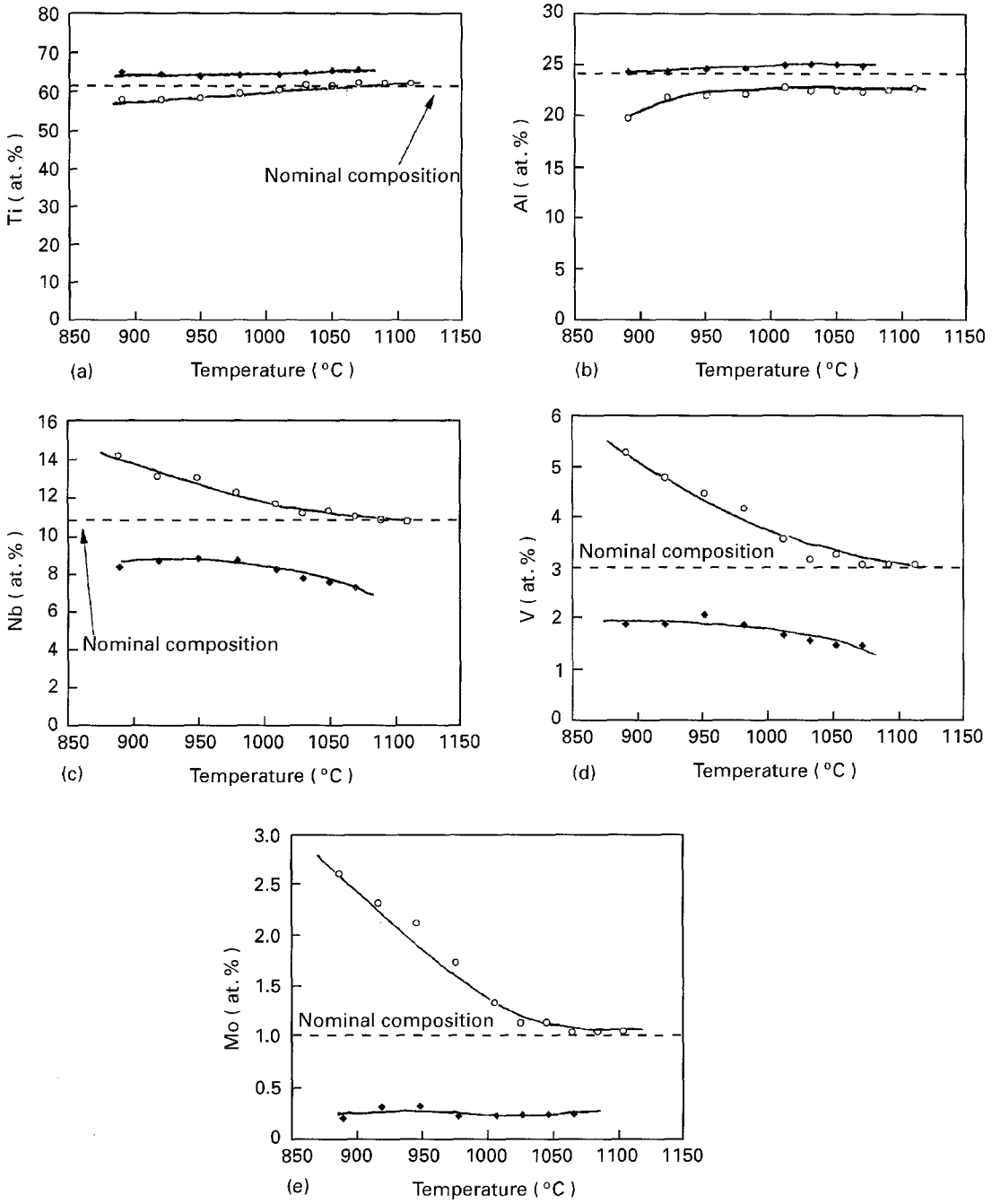

Figure 13 Variation with temperature of treatment of the compositions of (◆) α_2 and (○) β-phases: (a) titanium, (b) aluminium, (c) niobium, (d) vanadium, and (e) molybdenum.

tendency is observed in the β-phase for the three β stabilizing solutes: the amount of the element increases with decreasing temperature. This variation is significant in the case of niobium for which the concentration at $T = 890\,°C$ is approximately 1.5 times that at $T = 1070\,°C$. The variation is stronger in the case of vanadium for which the composition at 890 °C is nearly twice the nominal composition. The variation is even much more pronounced in the case of molybdenum, for which the composition at $T = 890\,°C$ is about three times the nominal composition. In order to know if a treatment of 24 h was long enough to reach thermodynamic equilibrium in the microstructure, two additional heat treatments were carried out at 890 and 920 °C for 96 h. WDS analyses were then performed on the corresponding water quenched specimens. They show that no significant further variation in composition of the α_2- or β-phase was obtained compared to the values corresponding to the 24 h heat treatments. It was consequently concluded that a 24 h holding time is sufficient to reach thermodynamic equilibrium in the investigated temperature domain.

4. Discussion

4.1. Expected superplastic properties of the as-received material

As mentioned earlier, the mean phase size (PS) is about 3 μm for the as-received material. This size can be compared to that of previously reported superplastic of Ti–25Al–11Nb–3V–1Mo (at %) alloys. Ghosh

and Cheng [2] reported linear intercept measurements equal to 10.2 μm in the longitudinal direction, 3.8 μm in the transverse direction and 1.3 μm in the thickness. According to the assumption made in this paper, these values lead to a mean phase size (PS) of 3.7 μm. Relatively comparable microstructures were demonstrated also to develop superplastic properties at $T \approx 980\,^{\circ}C$ [4]. The similar phase volume fractions for the α_2- and β-phases in the case of the investigated material were also generally reported for Ti_3Al based sheets to be formed by superplastic forming [2, 4]. As obtained in this study, heterogeneities in the distribution of the phases in the rolling plane of the sheet were already reported [4] and are associated with microstructures which have no preferential orientation in this plane, namely which undergo rolling in different directions. Care must then be taken during such hot rolling steps to limit, as much as possible, the development of such heterogeneities which may affect any further superplastic deformation.

As demonstrated by the X-ray diffraction profiles and the pole figures, the rolling steps induce a strong texture in the two phases of the material: a (1 0 0) [0 1 1] component for the β-phase and (1 1 $\bar{2}$ 0) [$\bar{1}$ 1 0 0] and (1 1 $\bar{2}$ 0) [0 0 0 1] components for the α_2-phase. This result confirms the previous ones obtained by Yu *et al.* [19] on a hot rolled (at a temperature close to 1000 °C) super α_2 alloy of 2.5 mm thickness. In the as-rolled condition, the same components were found in the α_2 and β-phases. In the case of conventional titanium alloys, the texture in the β-phase was demonstrated to affect both the superplastic behaviour and the mechanical properties after superplastic forming of the alloy [20–22]. However, texture is expected to decrease during deformation performed in the superplastic regime [23]. Consequently, the presence of a rolling-induced texture in the as-received alloy is not considered to be an insurmountable obstacle to achieve superplastic properties.

4.2. Effect of heat treatment on phase size and phase texture

Ti–25Al–10Nb–3V–1Mo (at %) alloys deformed superplastically at 980 °C can exhibit important strain hardening at low strain rates, e.g. $10^{-4}\ s^{-1}$, which has been interpreted in terms of significant phase growth confirmed by SEM observations of deformed samples [4]. The holding time at 980 °C during such tests does not exceed 10 h. This phase growth is due to static (maintain at high temperature) and dynamic (boundary migration enhanced by boundary sliding) contributions. As shown in Fig. 10, the increase of PS after 24 h at $T = 980\,^{\circ}C$ remains very limited (from 3.4 to 4.5 μm). This means that the contribution of dynamic grain growth to total grain growth during superplastic deformation performed at 980 °C is expected to be predominant. After heat treatment, the texture induced by rolling is roughly maintained in the whole investigated temperature domain.

4.3. Effect of heat treatment on variations in phase composition

In the case of two phase materials, the mechanical behaviour in superplastic conditions is generally described as a spatial reorganization of the two phases controlled, by plastic deformation in the softer phase, i.e. the β-phase for titanium alloys. This plastic deformation can result from dislocation activity or diffusion processes; but, in any case, the resulting constitutive law includes diffusion coefficients which operate in the soft phase. From this point of view, it can be of prime importance to estimate the effect of variations with the temperature of the composition of the soft phase. Variations of compositions in the α_2 and β-phases after annealing for 24 h in the temperature range 700–1000 °C have already been reported in the case of the Ti–24Al–11Nb–2V–1Mo (at %) alloy [14]. In this work and in the present paper, similar qualitative variations of the niobium contents in the α_2- and β-phases are obtained. In the case of the vanadium content, some differences between the two studies are observed. Morris and Morris [14] found that the vanadium contents are equal ($\simeq 2.3 \pm 0.3$ at %) in α_2 and β-phases and remain independent of temperature. In the case of the investigated alloy, significant enrichment in vanadium is observed in the β-phase, particularly at low temperature. This difference can be attributed to the higher nominal amount of vanadium (3.0 at % instead of 2.3 at %), associated with the low solubility limit of vanadium in the α_2-phase (less than 2.5 at % in the studied temperature domain). In the case of molybdenum, an important enrichment is observed in the β-phase at low temperature, which was not reported by Morris and Morris [14].

4.4. Effect of heat treatment on phase volume fractions

It has been well established that the phase volume fraction is a key parameter in the constitutive law of two phase materials in the superplastic regime [10]. The determination of the law of variation with temperature of phase volume fractions is then very important to foresee the temperature range in which superplastic properties can be expected. As shown in Fig. 12, an estimation of the variation with temperature of the α_2-phase volume fraction, $f_{vol}(\alpha_2)$, can be obtained from image analysis measurements performed on SEM micrographs. However, the determination of a phase volume fraction from data obtained in two-dimensional space (like the plane of observation) is a delicate problem, which may result in significant inaccuracies. Consequently, it is fruitful to try to obtain data concerning $f_{vol}(\alpha_2)$ by another technique, independent of the first one. Such a determination of $f_{vol}(\alpha_2)$ is possible from the knowledge of the α_2- and β- compositions in the investigated temperature domain, since the atomic phase fraction of α_2-phase, $f_{at}(\alpha_2)$, can be estimated by the application of the equilibrium law for each element according to

$$f_{at}(\alpha_2; i) = \frac{\overline{c(i)} - c_\beta(i)}{c_{\alpha_2}(i) - c_\beta(i)} \qquad (2)$$

where $c(i)$, $c_{\alpha_2}(i)$ and $c_\beta(i)$ are the concentration of element i in the alloy, α_2- and β-phase, respectively. The volume fraction of the α_2- phase can be identified with the atomic volume fraction if the unit cell volumes of the two phases are similar. From X-ray data, the lattice parameters of the two phases can be estimated for the alloy in the as-received condition. For the hexagonal α_2 structure, $a_{\alpha_2} = 0.5775$ nm and $c_{\alpha_2} = 0.4638$ nm, and for the cubic β-phase, $a_\beta = 0.3235$ nm. These values are in good agreement with those obtained by Wittenauer *et al.* [12], but are quite different for the α_2-phase from the results obtained by Morris and Morris [14]. They found $a_{\alpha_2} = 0.595$ nm and $c_{\alpha_2} = 0.467$ nm. However, it must be underlined that Wittenauer *et al.* have studied an alloy admitting a composition similar to that of the alloy investigated in the authors' study, whereas the composition of the material studied by Morris and Morris is slightly different. With the measured lattice parameters, cell volumes of the α_2- and β-phases can be calculated, according to $V_{cell}(\beta) = a_\beta^3$ and $V_{cell}(\alpha_2) = [3^{(1/2)}/2]\, a_{\alpha_2}^2 c_{\alpha_2}$. The difference between the cell volumes of the two phases is less than 2%. It can then be assumed that $f_{vol}(\alpha_2) \approx f_{at}(\alpha_2)$.

Equation 2 is as much accurate as the relative difference between α_2- and β-phase concentrations is important. For this reason, the data obtained for aluminium and titanium were not taken into account to calculate $f_{vol}(\alpha_2)$, since the concentrations in aluminium and titanium were shown to be quite similar in the α_2- and β-phases whatever the investigated temperature, as shown by Fig. 13a, b. Due to the low levels of molybdenum and vanadium in the alloy, the relative inaccuracies in the WDS measurements (Fig. 13d, e) can lead to significant errors in $f_{vol}(\alpha_2)$. For all these reasons, it was decided to calculate $f_{vol}(\alpha_2)$ from data obtained for niobium. In this framework, Equation 2 can be written

$$f_{vol}(\alpha_2) = \frac{\overline{c(\mathrm{Nb})} - c_\beta(\mathrm{Nb})}{c_{\alpha_2}(\mathrm{Nb}) - c_\beta(\mathrm{Nb})} \qquad (3)$$

Fig. 14 compares the variations with temperature of the α_2 volume fraction, estimated by image analysis and calculated from WDS data (Equation 3). A good agreement is obtained between the two curves obtained from independent techniques. Fig. 14 confirms that, for temperatures lower than 960 °C, the α_2 volume fraction varies only slightly during heat treatment in the case of the investigated material, whereas it decreases sharply at $T > 960$ °C.

As already mentioned, even if the processing route is not known in detail for the as-received material, it is likely that the rolling process includes steps in the β and (α_2 + β) fields. Therefore, the nodular α_2-phase observed in the as-received condition is mainly produced during the first steps in the two phase domain. It can be described as primary α_2^I phase. When additional heat treatment is carried out in the (α_2 + β) field, two phenomena can affect the microstructure. When the temperature of the treatment is higher than the temperature of the last steps of rolling, T_R, a decrease in the α_2^I-phase volume fraction occurs. When

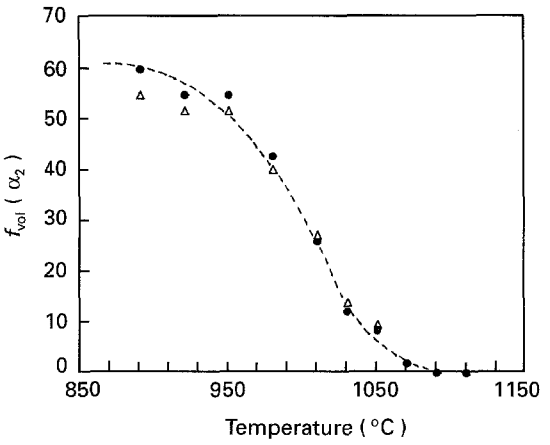

Figure 14 Comparison of the variation with temperature of $f_{vol}(\alpha_2)$ obtained from (△) image analysis data and (●) WDS measurements of niobium content.

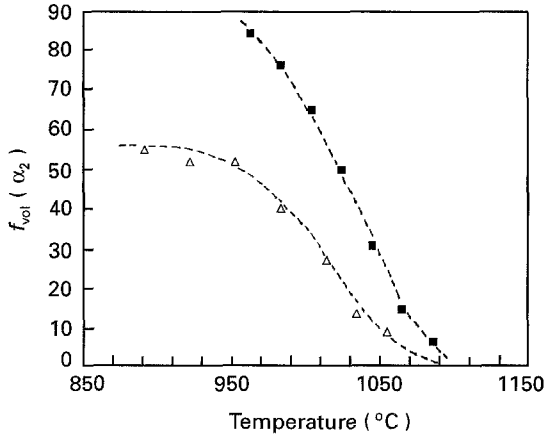

Figure 15 Variations with temperature of $f_{vol}(\alpha_2)$ in the case of (△) Ti–25Al–10Nb–1Mo–3V (at %) and (■) Ti–24Al–11Nb (at %) [1] alloys.

the temperature of the treatment is lower than T_R, a secondary α_2^{II}-phase is produced. The α_2^{II}-phase can coalesce with the α_2^I nodules and then increases the corresponding volume fraction of the α_2 nodules. It can also consist in the production of acicular phases, preferentially nucleated along β–β boundaries. It must be underlined that, as a result of the measurement techniques (image analysis and WDS), Fig. 14 shows only the variation with temperature of the volume fraction of the nodular α_2-phase. The two main effects of the heat treatment (shrinkage of α_2^I-phase and production of α_2^{II}-phase) correspond to the difference in the slope of $f_{vol}(\alpha_2)$. From this curve, it can be deduced that the last steps of rolling were carried out at $T_R \approx 950$ °C.

When $T > T_R$, the dependence on temperature of the α_2^I-phase volume fraction in the case of the Ti–25Al–10Nb–3V–1Mo (at %) alloy investigated can be compared with results published previously in the case of annealed Ti–24Al–11Nb (at %) specimens, having, in the as-received condition a fine (the grain size was about 4 μm) microduplex α_2–β microstructure [1]. Fig. 15 shows this comparison. At 980 °C, for which both materials exhibit superplastic properties, an important difference in phase volume fractions is

obtained: in the Ti–25Al–10Nb–3V–1Mo (at %) alloy, $f_{vol}(\alpha_2) \approx 40\%$ whereas $f_{vol}(\alpha_2) \approx 70\%$ in the Ti–24Al–11Nb (at %) alloy. The ability to maintain superplastic properties for so large an α_2-phase volume fraction in the case of Ti–24Al–11Nb (at %) alloy is attributed to the β-phase which progressively surrounds the α_2 grains [1]. This does not seem to occur in the case of the Ti–25Al–10Nb–3V–1Mo (at %) alloy [4]. The relatively low value of the slope of α_2 nodular shrinkage in the case of the Ti–25Al–10Nb–3V–1Mo (at %) alloy in reference to the Ti–24Al–11Nb (at %) alloy, can be attributed to the high content in molybdenum which is expected to hinder the transformation rate.

When $T < T_R$, an increase in the volume fraction of the nodular α_2-phase results from a decrease in the temperature of the treatment. Since this increase can only result from the production of α_2^{II}-phase, it indicates that coalescence between this phase and the initial α_2^I nodules takes place. It is probably also associated with a spheroidization of some α_2^{II} needles, particularly in the upper domain of the investigated temperature range.

4.5. Impact on superplastic behaviour

The law of variation with temperature of the α_2 volume fraction (Fig. 14) has been demonstrated to correspond to thermodynamic equilibrium, in relation with the as-received conditions, since analyses performed after 96 h heat treatment give similar results to those obtained after 24 h, which is approximately the maximum duration of a forming cycle (including possibly a diffusion bonding step). In order to estimate the amplitude of variation of $f_{vol}(\alpha_2)$ during deformation, additional treatment was carried out for 2 h at $T = 930\,°C$ and $T = 980\,°C$, which are the temperatures planned for superplastic forming. In these conditions, WDS analyses give similar results to those obtained after the corresponding heat treatment performed during 24 h. This means that, except at $T = 890\,°C$ for which complementary data would be required to conclude, the curve shown in Fig. 14 can be used to relate the strain rate sensitivity parameter, m, to $f_{vol}(\alpha_2)$ from its dependence on temperature (Fig. 16). This figure shows that the high value of m obtained at temperatures between 890 and 980 °C corresponds to a limited variation in α_2^I. In this temperature range, $f_{vol}(\alpha_2)$ varies from about 0.4 to 0.55. Optimum superplastic properties for the Ti–25Al–10Nb–3V–1Mo (at %) alloy are thus obtained for quite similar conditions as for conventional titanium alloys, namely for comparable volume fractions of the two phases.

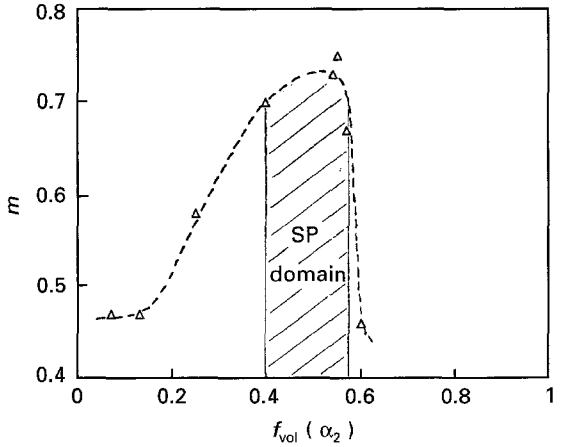

Figure 16 Variation of $f_{vol}(\alpha_2)$ with the maximum value of the strain rate sensitivity parameter, m_{max}, in the investigated strain rate domain.

5. Conclusions

The microstructures of a fine grained Ti–25Al–10Nb–3V–1Mo (at %) alloy have been studied in the as-rolled condition and after heat treatment. High temperature rolling produces relatively fine microduplex structures both with connected networks of α_2 and β-phases, but it is associated with significant textures in the material. After heat treatment carried out in the two phase field, it has been shown that as long as the two networks are connected, which corresponds roughly to $T \leqslant 980\,°C$, phase growth remains very limited and texture is maintained after treatment. The dependence on temperature of the compositions of the phases has been estimated. These variations occur mainly in the β-phase and preferentially concern the β stabilizing solutes. From two independent techniques, the variation with temperature of the volume fraction of the nodular α_2-phase has been determined and discussed in relation to the corresponding superplastic properties.

Acknowledgements

The authors acknowledge Dassault Aviation, Aérospatiale and Direction des Recherches, Etudes et Techniques (DRET) for financial support. They thank Dr M. Suery for helpful discussions.

References

1. A. DUTTA and D. BANERJEE, *Scripta Metall. Mater.* **24** (1990) 1319.
2. A. K. GHOSH and C. H. CHENG, in Proceedings of the International Conference on Superplasticity in Advanced Materials (ICSAM 91), May 1991, edited by S. Hori, M. Tokizane and N. Furushivo (Japan Society for Research on Superplasticity, Osaka, 1991) p. 299.
3. H. S. YANG, P. JIN, E. DALDER and A. K. MUKHERJEE, *Scripta Metall. Mater.* **25** (1991) 1223.
4. H. S. YANG, P. JIN and A. K. MUKHERJEE, *Mater. Sci. Eng.* **A153** (1992) 457.
5. H. S. YANG, M. G. ZELIN, R. Z. VALIEV and A. K. MUKHERJEE, *Scripta Metall. Mater.* **26** (1992) 1707.
6. M. T. COPE, D. R. EVETTS and N. RIDLEY, *J. Mater. Sci.* **21** (1986) 4003.
7. N. E. PATON and C. H. HAMILTON, in Proceedings of the Fifth International Conference on Titanium, September 1984, edited by G. Lütjering, U. Zwicker and W. Bunk, (Deutsche Gesellschaft für Metallkunde e.v., Munich, Germany,1984) p. 649.
8. J. WERT and N. E. PATON, *Metall. Trans.* **14A** (1983) 2535.
9. J. MA and C. HAMMOND, in Proceedings of the Fifth International Conference on Titanium, September 1984, edited by G. Lütjering, U. Zwicker and W. Bunk, (Deutsche Gesellschaft für Metallkunde e.v., Munich, Germany,1984) p. 703.

10. M. SUERY and B. BAUDELET, *Res. Mechanica* **2** (1981) 163.
11. Z. CHEN, F. SIMCA and M. T. COPE, *Mater. Sci. Technol.* **8** (1992) 729.
12. J. WITTENAUER, C. BASSI and B. WALSER, *Scripta Metall.* **23** (1989) 1381.
13. A. SZARUGA, M. SAGIB, R. OMLOR and H. A LIPSITT, *Scripta Metall. Mater.* **26** (1992) 787.
14. M. A. MORRIS and D. G. MORRIS, *Phil. Mag.* **63A** (1991) 1175.
15. H. T. WEYKAMP and D. R. BAKER, *Scripta Metall. Mater.* **24** (1990) 445.
16. A. W. THOMPSON and T. M. POLLOCK, *ISIJ Int.* **31** (1991) 1139.
17. W. CHO and W. THOMPSON, *Metall. Trans.* **21A** (1990) 641.
18. S. DJANARTHANY PhD thesis, Université Paris Sud, Paris (1992).
19. C. J. YU, D. ZHAO, J. J. VALENCIA and P. K. CHAUDHURY, *Mater. Res. Symp. Proc.* **288** (1993) 927.
20. O.A. KAIBYSHEV, I. V. KAZACHKOV and R. M. GALEEV, *J. Mater. Sci.* **16** (1981) 2501.
21. D.S. McDARMAID, A. W. BOWEN and P. G. PARTRIDGE, *ibid.* **19** (1984) 2378.
22. M. T. COPE, D. R. EVETTS and N. RIDLEY, *Mater. Sci. Technol.* **3** (1987) 455.
23. A. W. BOWEN, D. S. McDARMAID and P. G. PARTRIDGE, *J. Mater. Sci.* **26** (1991) 3457.

Received 2 February
and accepted 11 May 1995